Contents lists available at ScienceDirect

Genomics

journal homepage: www.elsevier.com/locate/ygeno

GENOMICS

Characterization and functional analysis of *cis*-acting elements of the human farnesyl diphosphate synthetase (FDPS) gene 5′ flanking region

Maria Grazia Romanelli *, Pamela Lorenzi, Antonella Sangalli, Erica Diani, Monica Mottes

Department of Mother and Child, Biology and Genetics, University of Verona, Strada le Grazie 8, 37134 Verona, Italy

ARTICLE INFO

ABSTRACT

Farnesyl diphosphate synthetase (FDPS) is a key enzyme in the isoprenoid pathway responsible for cholesterol biosynthesis, post-translational protein modifications and synthesis of steroid hormones, whose expression is regulated by phorbol esters and polyunsaturated fatty acids.

Genomic comparison of the 5′ upstream sequence of the FDPS genes identifies conserved binding sites for NF-Y, SP1, SRE3, and YY1 regulatory elements in rat, mouse, dog and chimpanzee. Two additional specific consensus sequences, upstream of the core promoter that had not been analysed previously, are shared only by human and chimpanzee genomes.

The work presented here aimed at characterizing these genomic sequence elements in the human FDPS promoter region and their contribution to gene expression. We have characterized functionally the minimal basal promoter of the human FDPS gene by means of deletion mutants and we have identified two *cis*-acting elements which modulate the FDPS gene expression and are recognized by Pax5 and OCT-1 transcription factors.

© 2008 Elsevier Inc. All rights reserved.

Introduction

Farnesyl diphosphate synthetase (FDPS; EC 2.5.1.1/EC 2.5.1.10) is a polyprenyltransferase that catalyzes the synthesis of farnesyl pyrophosphate (FPP) by the sequential 1′–4 condensation of dimethilallyl diphosphate with two molecules of isopentenyl diphosphate. [1]. FDPS is a key enzyme in isoprenoid biosynthetic pathway. The product of its catalytic activity, FPP, is a common intermediate in the synthesis of both sterol and non-sterol isoprenoid compounds. They are represented by cholesterol, ubiquinone, dolichol, and metabolites necessary for post-translational prenylation of small GTPases that are involved in cell growth and survival, motility, cytoskeletal regulation, intracellular transport, and secretion [2–5]. Given the essential role of this pathway in several clinical conditions, new drugs have been developed to inhibit the activity of the key enzymes in the isoprenoid synthesis, such as statins which inhibit the hydroxymethylglutaryl-CoA reductase (HMGCR) to lower cholesterol levels, or farnesyl transferase inhibitors (FTIs) for the treatment of cancer [6]. FDPS activity, in particular, is inhibited by nitrogen-containing bisphosphonates (N-BPs), that are used as bone antiresorptive drugs in disorders such as osteoporosis, Paget disease, or multiple myeloma [7,8]. FDPS is most likely the molecular target of N-BPs, synthetic analogues of inorganic

pyrophosphate [9]. N-BPs are potent inhibitors of FDPS [10–14] and prevent the synthesis of prenilated proteins involved in the regulation of a variety of osteoclast cell processes, including cytoskeletal arrangement, membrane ruffling, trafficking of intracellular vesicles and apoptosis [15–18]. Studies in *Dictyostelium discoideum* have demonstrated that over-expression of FDPS leads to resistance to the growth-inhibitory effect of N-BPs [12,19]. The expression of human and rat FDPS gene has been demonstrated to be regulated by phorbol esters [20]. Dietary polyunsaturated fatty acids (PUFAs) suppress transcription of hepatic FDPS, acting on lipogenic transcriptional factor SREBP-1c (SREBF1) and modulating NF-Y binding to regulatory elements in the promoter region [21,22]. FDPS is an alternatively spliced gene encoding for at least two major isoforms in eukaryotes: one is localized in peroxisomes, despite its lack of a peroxisome targeting sequence [23]; a second one is a mitochondrial isoform that has been detected in humans, fruit flies and plants [24,25]. FDPS genes have been recently characterized in basidiomycetus fungus [26]. Variations in the FDPS enzyme activity have been related to human diseases. A reduced activity of FDPS has been demonstrated in the hepatic tissue of patients with peroxisomal disorders such as Zellweger disease and neonatal adrenoleukodystrophy [27]. In addition, preliminary results associate a single nucleotide polymorphism in the FDPS gene to lower bone mineral density in postmenopausal Caucasian women [28]. Functional analysis of the promoter region of the gene has been performed in rat. In this animal model, FDPS gene encodes different mRNA transcripts that show different translational efficiency, tissue distribution and transcriptional regulation. Two major representative rat FDPS mRNAs

* Corresponding author. Dipartimento Materno Infantile e di Biologia-Genetica, Sezione di Biologia e Genetica, Universita' degli Studi di Verona, Strada le Grazie, 8, 37134 Verona, Italy. Fax: +39 045 8027180.
E-mail address: mariagrazia.romanelli@univr.it (M.G. Romanelli).

differing in the length of the 5′ untranslated region, are expressed with tissue specificity in liver and testis [29]. The promoter contains canonical TATA and CCAAT boxes and several consensus sequences of the sterol-regulatory elements (SRE-1) [30]. Additional regulatory factors that are involved in the sterol-mediated transcriptional regulation have been identified. A 6 base-pair sequence ATTGGC recognized by either NF-Y or Sp1 transcription factors has been demonstrated to be necessary for sterol regulation in the rat FDPS [31,32]. A second element, termed SRE-3, is required both for sterol-regulated transcription and for binding of sterol regulatory element binding protein 1 (SREBP-1) [33,34], whereas a negative regulator of FDPS transcription has been identified as Yin and Yan 1 protein (YY1) [35]. To date human FDPS gene expression has been poorly characterized, therefore the current investigations were designed to specifically characterize the human FDPS gene promoter. We have cloned the 5′-flanking region of the human FDPS gene and characterized two cis-

acting sequences, not investigated previously, which are highly conserved in human and chimpanzee FDPS gene upstream sequences.

Material and methods

RT-PCR

Multiple Tissue cDNA panels (MTC™ panel I and II, BD Biosciences Clontech) were utilized for semi-quantitative FDPS expression analysis by polymerase chain reaction (PCR) [36]. MTC™ panels I and II consist of first-strand cDNAs generated using Oligo-dT by poly $(A)^+$RNA isolated from sixteen different human tissues: heart, brain, placenta, lung, skeletal muscle, liver, kidney and pancreas for panel I; thymus, spleen, prostate, testis, small intestine, ovary, peripheral blood leucocytes and colon for panel II, respectively. The cDNA preparations are normalized to the mRNA expression levels of four
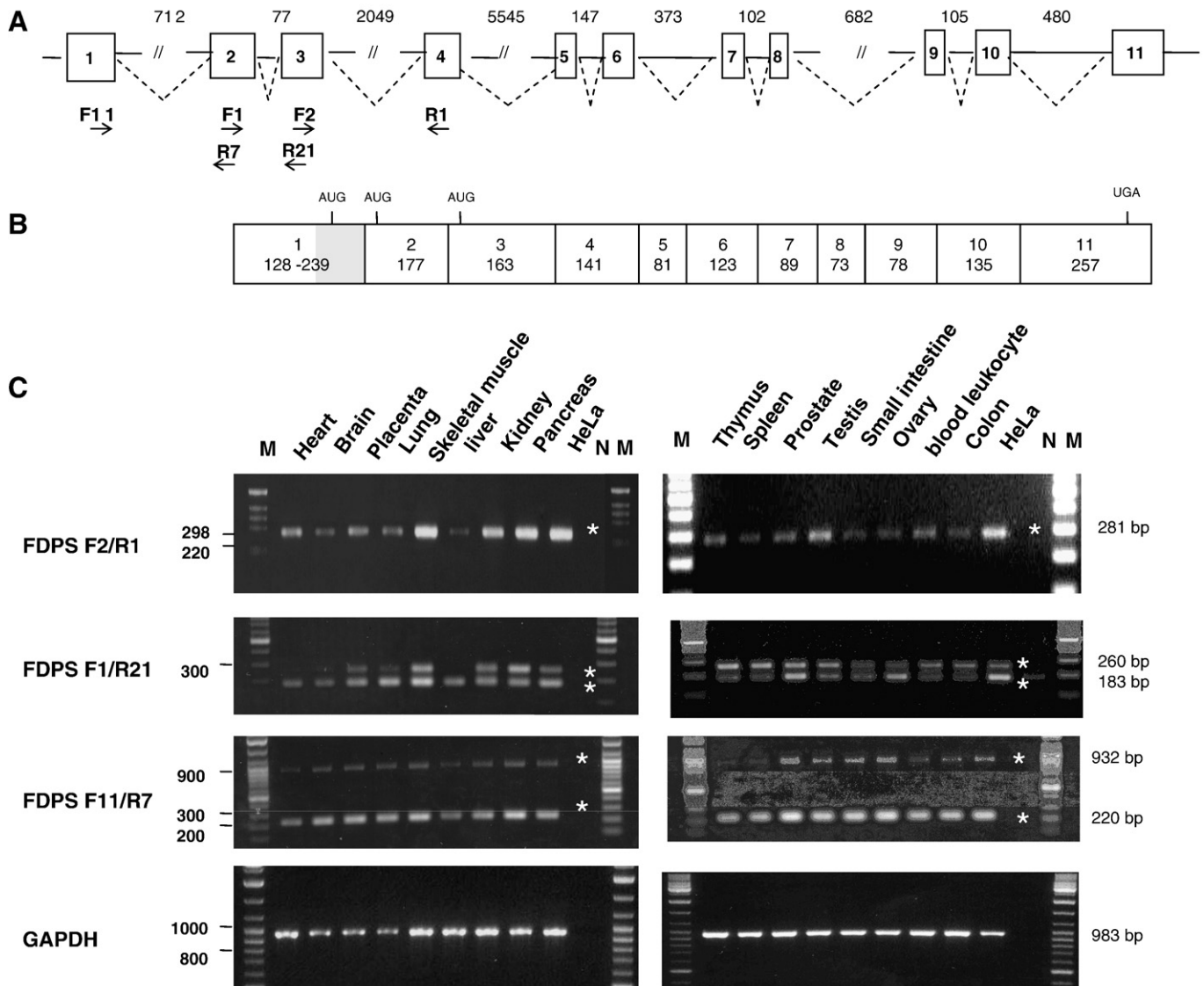

Fig. 1. Structure of the human FDPS gene and expression pattern of FDPS mRNA in human tissues. (A) Exon–intron structure of the human FDPS gene was deduced by MGAlignIt using accession numbers NM_002004 and NT_004487; the numbers above horizontal lines indicate the introns length; (B) Schematic representation of exons (1 to 11); alternative exon extension is gray-shadowed; exon sizes are indicated inside the boxes. (C) Bioscience Clontech derived from poly(A)+ RNA extracted from heart, brain, placenta, lung, liver, skeletal muscle, kidney, pancreas, thymus, spleen, prostate, testis, small intestine, ovary, peripheral blood leukocyte colon human normal tissues, and HeLa cells were analyzed by performing PCR amplifications using FDPS specific primer pairs. FDPS F2/R1: the predicted 281 bp PCR product was amplified with primers complementary to exon 3 and 4 sequences, using 38 cycles of amplification. FDPS F1/R21: the predicted 260or 183 bp products were amplified with primers complementary to exon 1 and exon 2 sequences. FDPS R11/R7 932 and 220 bp PCR products were amplified with primers complementary to exon 2 and exon 3 sequences. GAPDH: the ~1 kb GAPDH product of amplification obtained from the same tissue panel was included as a control for RNA quality and normalization. DNA size markers are shown in lane M (1 kb ladder for panel F2/R1, and Gene ruler for panels F1/R21, F11/R7 and GAPDH); N, control PCR reaction with no added template.

different housekeeping genes: α tubulin, β actin, glyceraldehyde-3-phosphate dehydrogenase (GAPDH) and phospholipase A2. FDPS specific primers were the following: primers F1, F2, R1 and R7 and R21, complementary to sequences in exon 2, 3 (F) and sequences in exon 4, 2 and 3 (R), respectively, were derived by mRNA sequence GenBank accession no. NM_002004. Primer F11 complementary to sequences in exon 1 was derived by contig entry GenBank accession no. NT_004487. Primer positions are schematically indicated in Fig. 1 panel A, their sequences are listed in Table 1. PCR cycling conditions were 20 s at 95 °C, 20 s at 62 °C, 1 min at 72 °C for 34 cycles and a final extension for 3 min at 72 °C. Sense 5′-TGAAGGTCGGAGTCAACGGATTTGGT-3′ and antisense 5′-CATGTGGGCCATGAGGTCCACCAC-3′ primers, specific to GAPDH sequences, were used in control analysis for tissue expression pattern of a housekeeping gene, according to the manufacturer's recommendations. Aliquots of each amplified product taken after 28, 30, 35 or 38 cycles, respectively, were analyzed by electrophoresis on 1.5 or 3% agarose gels and visualized by SYBR Safe DNA gel stain (Invitrogen). All the PCR products were sequenced and analyzed by sequence alignment to the reference genomic sequence.

Cloning of the 5′-flanking region of the human FDPS

A 5′-upstream region of the human FDPS gene was amplified by PCR from human genomic DNA with F3 and R2 primers (Table 1) derived by contig entry GenBank accession no. NT_004487 genomic sequences and positioned at −718 and +118 relative to the first nucleotide in the mRNA sequence reported in NM_002004, respectively. Hind III and Kpn I restriction endonuclease recognition sites were introduced at their ends. We used the following cycling conditions: initial denaturation at 95 °C for 5′, 30 cycles at 95 °C for 20 s, annealing temperature decreasing 1° every second cycle from 72 °C to 56 °C for 20 s, 72 °C for 1′, further 15 cycles at 95 °C for 20 s, 56° for 20 s, 72° for 1′, and final extension at 72 °C for 5′. A fragment of 819 bp was amplified and cloned into pGL3-basic vector (Promega). The isolated and cloned genomic fragment was sequenced at the BMR Genomics facility (http://www.bmr.genomics.it).

In silico analysis of the promoter region

Exon–intron structure of the human FDPS gene was partially deduced by MGAlignIt at site http://origin.bic.nus.edu.sg/mgalign/mgalignit [37]. Splice sites and alternative splice sites were obtained by application of the following programs: Splice site prediction by Neural Network at BDGP (Berkeley Drosophila Genome Project, www.fruitfly.org/seq_tools/splice.html) [38]; ASSP (alternative splice site predictor at web site: www.es.embnet.org/~mwang/assp.html) [39], and NetGen2 server at web site: www.cbs.dtu.dk/services/NetGene2/ [40,41]. The genomic sequence of 819 bp upstream the FDPS gene was analyzed for putative promoter sequence using PromoterInspector software at site http://www.genomatix.de/cgi-bin/eldorado/main.pl and for potential transcription binding using TRANSFAC Transcription Factor Binding Sites Database [42] at site http://www.gene-regulation.com/ and MatInspector at site http://www.genomatix.de/cgi-bin/eldorado/main.pl. Alignments of the genomic sequences from human, mouse, rat, chimpanzee and dog were derived by BLAST and BLAT [43] analyses, carried out comparing the upstream sequences of FDPS against genomic sequences from a range of organisms in the database at http://www.ncbi.nlm.nih.gov/blast/Blast.cgi and the genome browser at http://genome.ucsc.edu.

Promoter constructs and deletion mutants

A series of human FDPS promoter–luciferase constructs was generated by PCR using the 819 bp cloned genomic fragment as template, a common antisense primer R2 containing a Hind III restriction site and, alternatively, the F3, F4, F6 and F14 sense primers containing a Kpn I restriction site (Fig. 2). The PCR products were digested with Hind III and Kpn I and, successively, sub-cloned into pGL3-Basic Vector (Promega) containing the luciferase reporter gene. In order to delete the ATAATGAAAA sequence relative to the putative OCT-1 (POU2F1) cis-element at position −382 into the pGL3 −718/+118 construct, we used the F7 Δ OCT-1 and R4 Δ OCT-1 mutated primers. The sequence relative to the putative Pax5 (PAX5) cis-element at position-249 was mutagenized from the pGL3 −718/+118 construct using the F8 ΔPax5 and R5 ΔPax5 mutated primers lacking the CCACAGTGC sequence. A construct deleted in both OCT-1 and Pax5 putative cis-elements was generated introducing the Pax5 mutation in the OCT-1 deleted mutant. A promoterless clone [−60/+118] was created with primers F14/R2 from the pGL3 −382/+118 construct. PCR products were digested with Hind III and Kpn I and sub-cloned in pGL3-Basic vector. Primers sequences are shown in Table 1. Each construct was sequenced from both ends in order to check the correct orientation and fidelity.

Cell culture

Adherent HeLa cells were maintained in exponential growth in Dulbecco's modified Eagles medium (Cambrex) supplemented with 10% fetal calf serum (Cambrex), glutamine (2.0 mM), and gentamycin (50 μg/ml) at 37 °C in 5% CO_2.

Transient cell transfection and luciferase assay

24 h before transfection, cells were plated in a 24-wells plate at a density of 8×10^4 cells/well, and allowed to grow under normal culture conditions. Promoterless firefly luciferase reporter vector pGL3-basic was used as a negative control in all assays. 1 ng of the plasmid phRL-TK (Promega) containing the Renilla firefly gene and 0.6 μg of pGL3-reporter vectors containing the FDPS promoter sequences were co-transfected in each well using Polyfect reagent (Quiagen). Transfected cells were harvested 24 h later with Dual-Luciferase Reporter Assay System buffer (Promega) and luciferase activity was measured in each cell lysate by luminometry. FDPS promoter–luciferase activity in transfected cells was normalized to Renilla luciferase activity derived from the phRL-TK vector. Data were analyzed as fold expression relative to luciferase activities of the promoterless pGL3-Basic vector. All assays were performed at least three times in triplicate. Results are presented as mean±SD. Statistical significance was determined using the Student's t-test. A p-value of <0.05 was considered significant.

Table 1
Primer pairs for PCR and mutagenesis

Prime name	Position[a,b]	Primer sequence
F1	+24 to +42[a]	5′-TGGTTGAGATCTGTGGGGGTCT-3′
F2	+207 to +229[a]	5′-ATGAACGGAGACCAGAATTCAG-3′
F3	−718 to −696[b]	5′-**TCGGGTACC**GTATTTTTAGTAGAGACGGGGT-3′
F4	−364 to −343[b]	5′-**TCGGGTACC**AGACAGGCAGCCAAAGCCACAG-3′
F6	−382 to −361[b]	5′-**TCGGGTACC**ATAATGAAAACTTGAGTAAGAC-3′
F7 Δ OCT-1	−397 to −358[b]	5′-CAGCTGCCCAGGAAGCTTGAGTAAGACAGG-3′
F8 Δ Pax5	−264 to −225[b]	5′-TCGTCCGTCACAGTGCCATGCTCACACGAC-3′
F11	+73 to +92[b]	5′-ATACTGTGAGGCATCGGAAG-3′
F14	−60 to −41[b]	5′-**CATGGTACC**GCGGATTCTGCTTTTAGGAG-3′
R1	+466 to +488[a]	5′-CAGTTCCACACACGCCCCACA-3′
R2	+98 to +118[a]	5′-**CTCAAGCTTC**TTCAAAACGGACACAACAG-3′
R4 Δ OCT-1	−358 to −397[b]	5′-CCTGTCTTACTCAAGCTTCCTGGGCAGCTG-3′
R5 Δ Pax5	−225 to −264[b]	5′-GTCGTGTGAGCATGGCACTGTGACGGACGA-3′
R7	+984 to +1004[b]	5′-GGTTCCTCTGTCCACGCTTG-3′
R21	+206 to +187[a]	5′-TCTGAGGGAGGAGCAAAGGG-3′

[a] Positions are relative to nucleotides numeration of the mRNA sequence ref. GenBank accession no. NM_002004 mRNA (positive numeration).

[b] Positions are relative to the distance from the first nucleotide of the mRNA sequence ref. GenBank accession no. NM_002004, derived by contig sequence GenBank accession no. NT_004487. Bold characters indicate the sequence relative to the restriction sites introduced at the primers ends.
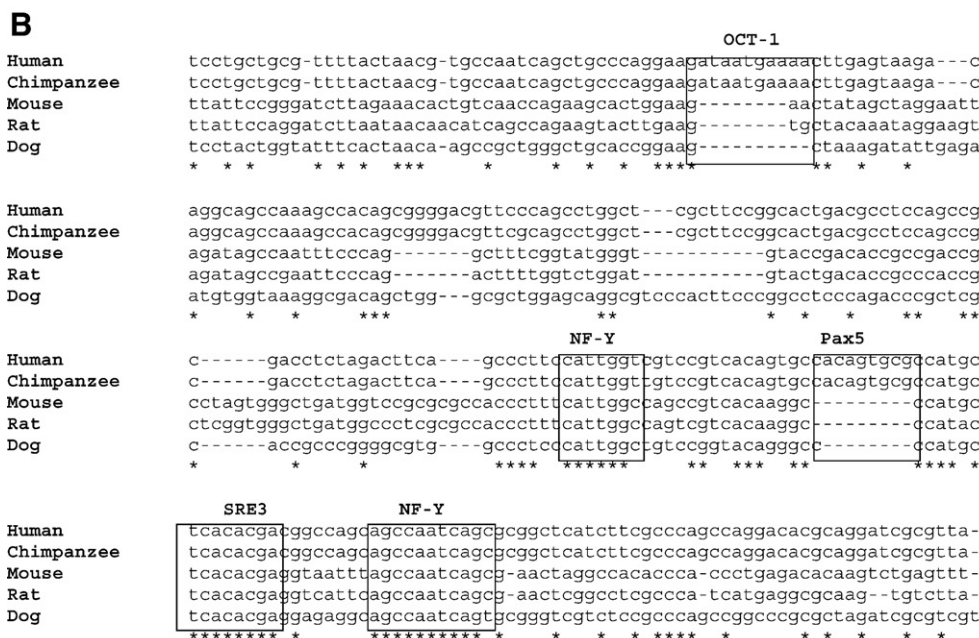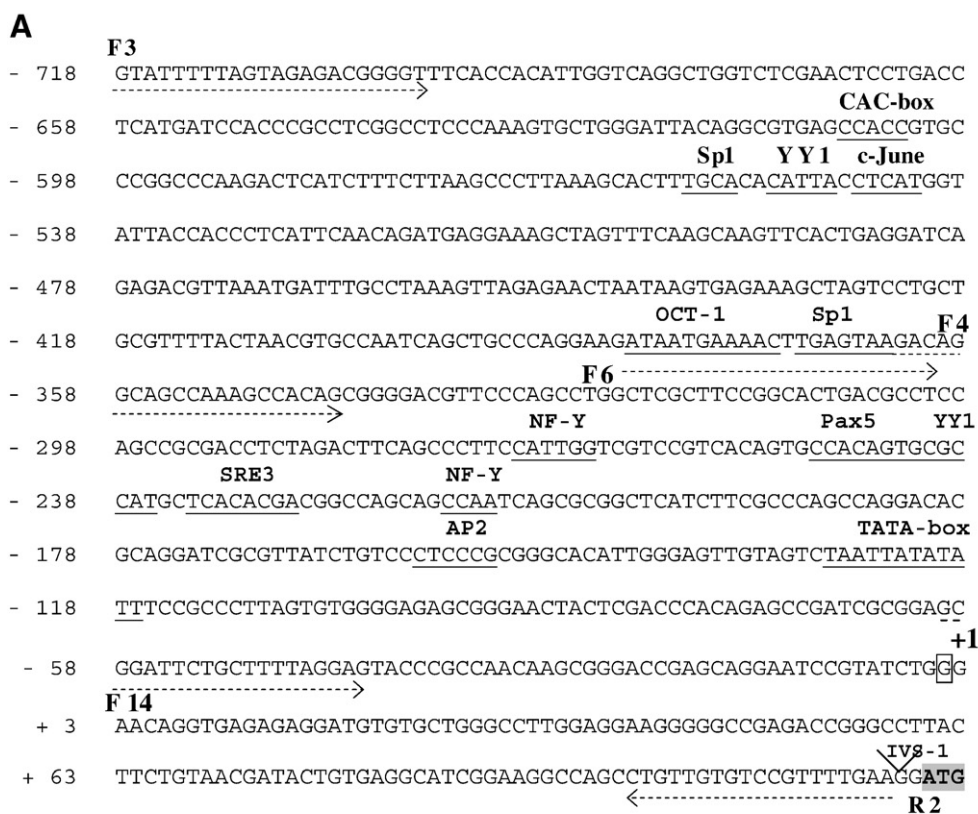
A

```
         F 3
  - 718  GTATTTTTAGTAGAGACGGGGTTTCACCACATTGGTCAGGCTGGTCTCGAACTCCTGACC
        ------------------------------->
                                                          CAC-box
  - 658  TCATGATCCACCCGCCTCGGCCTCCCAAAGTGCTGGGATTACAGGCGTGAGCCACCGTGC
                                       Sp1      Y Y 1   c-June
  - 598  CCGGCCCAAGACTCATCTTTCTTAAGCCCTTAAAGCACTTTGCACACATTACCTCATGGT

  - 538  ATTACCACCCTCATTCAACAGATGAGGAAAGCTAGTTTCAAGCAAGTTCACTGAGGATCA

  - 478  GAGACGTTAAATGATTTGCCTAAAGTTAGAGAACTAATAAGTGAGAAAGCTAGTCCTGCT
                                       OCT-1          Sp1        F4
  - 418  GCGTTTTTACTAACGTGCCAATCAGCTGCCCAGGAAGATAATGAAAACTTGAGTAAGACAG
                                      F 6 ------------------------------->
  - 358  GCAGCCAAAGCCACAGCGGGGACGTTCCCAGCCTGGCTCGCTTCCGGCACTGACGCCTCC
        ------------------------->
                                       NF-Y              Pax5      YY1
  - 298  AGCCGCGACCTCTAGACTTCAGCCCTTCCATTGGTCGTCCGTCACAGTGCCACAGTGCGC
                   SRE3                  NF-Y
  - 238  CATGCTCACACGACGGCCAGCAGCCAATCAGCGCGGCTCATCTTCGCCCAGCCAGGACAC
                         AP2                             TATA-box
  - 178  GCAGGATCGCGTTATCTGTCCCTCCCGCGGGCACATTGGGAGTTGTAGTCTAATTATATA

  - 118  TTTCCGCCCTTAGTGTGGGGAGAGCGGGAACTACTCGACCCACAGAGCCGATCGCGGAGC
                                                                      +1
  -  58  GGATTCTGCTTTTAGGAGTACCCGCCAACAAGCGGGACCGAGCAGGAATCCGTATCTGGG
        ----------------------------->
         F 14
  +   3  AACAGGTGAGAGAGGATGTGTGCTGGGCCTTGGAGGAAGGGGGCCGAGACCGGGCCTTAC
                                                               IVS-1
  +  63  TTCTGTAACGATACTGTGAGGCATCGGAAGGCCAGCCTGTTGTGTCCGTTTTGAAGGATG
                                              <-----------------------------
                                                                      R 2
```

B

```
                        OCT-1
Human      tcctgctgcg-ttttactaacg-tgccaatcagctgcccaggaagataatgaaaacttgagtaaga---c
Chimpanzee tcctgctgcg-ttttactaacg-tgccaatcagctgcccaggaagataatgaaaacttgagtaaga---c
Mouse      ttattccgggatcttagaaacactgtcaaccagaagcactggaag--------aactatagctaggaatt
Rat        ttattccaggatcttaataacaacatcagccagaagtacttgaag---------tgctacaaataggaagt
Dog        tcctactggtatttcactaaca-agccgctgggctgcaccggaag----------ctaaagatattgaga
           *  *  *      * * *  ***    *      * * *  ****        ** * * *

Human      aggcagccaaagccacagcggggacgttcccagcctggct---cgcttccggcactgacgcctccagccg
Chimpanzee aggcagccaaagccacagcggggacgttcccagcctggct---cgcttccggcactgacgcctccagccg
Mouse      agatagccaatttcccag-------gctttcggtatgggt-----------gtaccgacaccgccgaccg
Rat        agatagccgaattcccag-------acttttggtctggat-----------gtactgacaccgcccaccg
Dog        atgtggtaaaggcgacagctgg---gcgctggagcaggcgtcccacttcccggcctcccagacccgctcg
           *      *     ***              **          *  *     **  **   **

                             NF-Y              Pax5
Human      c------gacctctagacttca----gcccttccattggtcgtccgtcacagtgccacagtgcgccatgc
Chimpanzee c------gacctctagacttca----gcccttccattggtcgtccgtcacagtgccacagtgcgccatgc
Mouse      cctagtgggctgatggtccgcgcgcgccacccttccattggccagccgtcacaaggc--------ccatgc
Rat        ctcggtgggctgatggccgcgccgcgccaccctttccattggccgtccggtacagggcc-------ccatac
Dog        c------accgccgggggcgtg----gccctccattggccgtccggtacagggcc--------ccatgc
           *        *       *           ****  ****** **  *** **     ****  *

           SRE3              NF-Y
Human      tcacacgacggccagcagccaatcagcgcggctcatcttcgcccagccaggacacgcaggatcgcgtta-
Chimpanzee tcacacgacggccagcagccaatcagcgcggctcatcttcgcccagccaggacacgcaggatcgcgtta-
Mouse      tcacacgaggtaatttagccaatcagcg-aactaggccacaccca-ccctgagacacaagtctgagtttt-
Rat        tcacacgaggtcattcagccaatcagcg-aactcggcctgacca-tcatgaggcgcaag--tgtctta-
Dog        tcacacgaggagaggcagccaatcagtgcgggtcgtctccgcccagccggcccgcgctagatcgcgtcgt
           ********* *    ********** *    *    * * **** **   *   *  * * *
```

Fig. 2. Nucleotide sequences of the 5′-flanking region of the human FDPS and sequence alignment of FDPS orthologs. (A) 5′ upstream FDPS gene human genomic sequence. Putative transcription factor-binding sites and cis-acting elements are underlined and labelled: CAC-box, Sp1, YY1, c-June, OCT-1, Sp1, NF-Y, Pax5, SRE3, AP2, TATA-box. The firs nucleotide in the mRNA sequence in GeneBank NM_002004 is indicated as +1 and framed. The intron 1 sequence is indicated as IVS-1. Primers utilized in PCR amplifications to produce constructs pGL3 −718, −382, −364, or −60/+118 are indicated by dotted arrows. The ATG codon indicating the translation start site is in grey. (B). Multiple alignment of genomic upstream sequences of FDPS orthologs. Alignments obtained by BLAT analyses of genomic human, chimpanzee, rat, mouse and dog sequences are shown. Asterisks indicate nucleotides identity in all aligned sequences. Putative transcription binding site for OCT-1, NF-Y, Pax5 and SRE3 factors are framed.

Chromatin immunoprecipitation (Chip) assay

To determine the binding of OCT-1 and Pax5 factors to FDPS promoter, ChIP assays were performed with the EpiQuik™ Chromatin Immunoprecipitation kit based on the protocol provided by the supplier (Epigentek Group Inc., Brooklyn, NY). Immunoprecipitations were performed on samples of 1×10^6 HeLa cells. Cellular components were cross-linked by incubation of HeLa cells with 1% formaldehyde at room temperature for 10′; the reaction was stopped by addiction of glycine (final concentration 125 mM). Nuclei were extracted by centrifugation

after incubation of the sample with a pre-lysis buffer on ice for 10′; the pellet was resuspended in a lysis buffer with a protease inhibitor cocktail and incubated on ice for 10′. DNA was sheared by sonication (4 pulses of 10 s at 14 μm Amplitude with an MSE Soniprep 150 Ultrasonic disintegrator) to produce fragments between 200–1000 bp. After centrifugation, cell debris was discarded; an aliquot of DNA-containing supernatant was analyzed on agarose gel to check the shearing of DNA samples. An aliquot of DNA-containing supernatant was removed as "input" DNA and stored on ice. DNA samples diluted with ChIP dilution buffer were transferred into the strip wells previously precoated with the antibody against human OCT-1 (Santa Cruz Biotechnology, Inc.), Pax5 (Abcam), RNA polymerase II (Abcam), or non specific mouse IgG (a negative control provided by the kit supplier), respectively. Incubation was at room temperature for 90′ on an orbital shaker at 100 rpm. Wells were washed 6 times with a wash buffer (allowing 2′ on an orbital shaker at 100 rpm for each wash) and once with TE buffer (Tris–HCl, pH 8, 1 mM EDTA). Precipitated DNA–protein complexes and the input sample were treated with proteinase K (250 μg/ml) and the DNA release buffer for 15 min at 65 °C and subsequently incubated in reverse buffer for 90′ at 65 °C to obtain the cross-linked DNA reversal reaction. DNA samples were finally collected by spin column, washed with 70% and 90% ethanol and then eluted from the column with the elution buffer. Purified DNAs were analysed by PCR utilizing primers specific for FDPS promoter regions relative to the OCT-1 and Pax5 putative *cis*-acting signals, respectively. PCR assays were performed using the GoTaq® Mastermix (Promega) under the following condition: hot start at 95 °C for 2′, denaturation 95 °C for 30 s, annealing at 57 °C for 30 s, extension at 72 °C for 30 s and final extension at 72 °C for 5′. Primers specific for the predicted OCT-1 and Pax5 consensus region in the FDPS promoter were: *ChIP_Oct1-1F* 5′-TGCTGCGTTTTACTAACGTG-3′ and *ChIP_Oct1-1R* 5′-CAATGGAAGGGCTGAAGTC-3′; *ChIP_Pax5-1F*: 5′-GAGTAAGACAGG-CAGCCAAA-3′ and *ChIP_Pax5-1R*: 5′-GGACAGATAACGCGATCCT-3′. Primers for the RNA polymerase II binding region in the GAPDH promoter (positive control) were the following: *GAPDH-F*: 5′-GAGCGGTGCTGGGC-TCCGGCTCC-3′ and *GAPDH-R*: 5′-GCAGCAGGACACTAGG-3′. Primers for a chromosome 16 centromere (16cen) region (negative control) were

the following: *16cen*-F: 5′-GTCTCTTTCTTGTTTTTAAGCTGGG-3′ and *16cen-R* 5′-TGAGCTCATTGAGACATTTGG-3′. PCR products were analysed on a 2% agarose gel, stained with ethidium bromide and visualized on a UV transilluminator.

Results and discussion

FDPS gene organization and mRNA expression in human tissues

A human FDPS cDNA coding for a putative protein of 353 amino acids has been initially isolated by screening human hepatoma cell line (HepG2) and placental cDNA libraries [20]. A longer transcript, 1345 bp in length that codifies for a peptide of 419 amino acids is actually attributed to the mRNA sequence of human FDPS gene deposited into GenBank entry NM_002004. These two peptides have been recently described as isoforms of the same FDPS enzyme with specific sub-cellular distributions: one is detected preferentially into the peroxisomes and another, containing an N-terminal extension of 66 amino acids, is destined to the mitochondria [25]. This specific dual sub-cellular localization of the FDPS enzyme seems to be widespread among eukaryotes [25]. The human FDPS gene maps on chromosome 1q22 with location starting at 153,545,267 (NC 000001.9) and extending for 11,814 nucleotides. Ten related pseudo-genes have been recognized in the human genome, mapping on six different chromosomes [44,45], A. F. Scott, Personal communications, 11/9/2006, Baltimore, MD]. Multiple transcription start sites have been identified in the 5′ region of human FDPS by 5′ RACE [20,25]. Few studies have attempted to describe the complex organization of the 5′ region of the gene. A detailed study of "Martin et al. [25]" indicates that at least three different transcription start sites can be positioned at −136, −36, and −29, respectively, relative to the first ATG codon in exon 1. From both the genomic information (NT_004487) and the mRNA sequence (NM_002004) relative to FDPS sequence deposited in the NCBI database we derived a map of the exon–intron boundaries of the gene applying the MGAlignIt algorithm. A summary of the genomic organization and splicing pattern of the
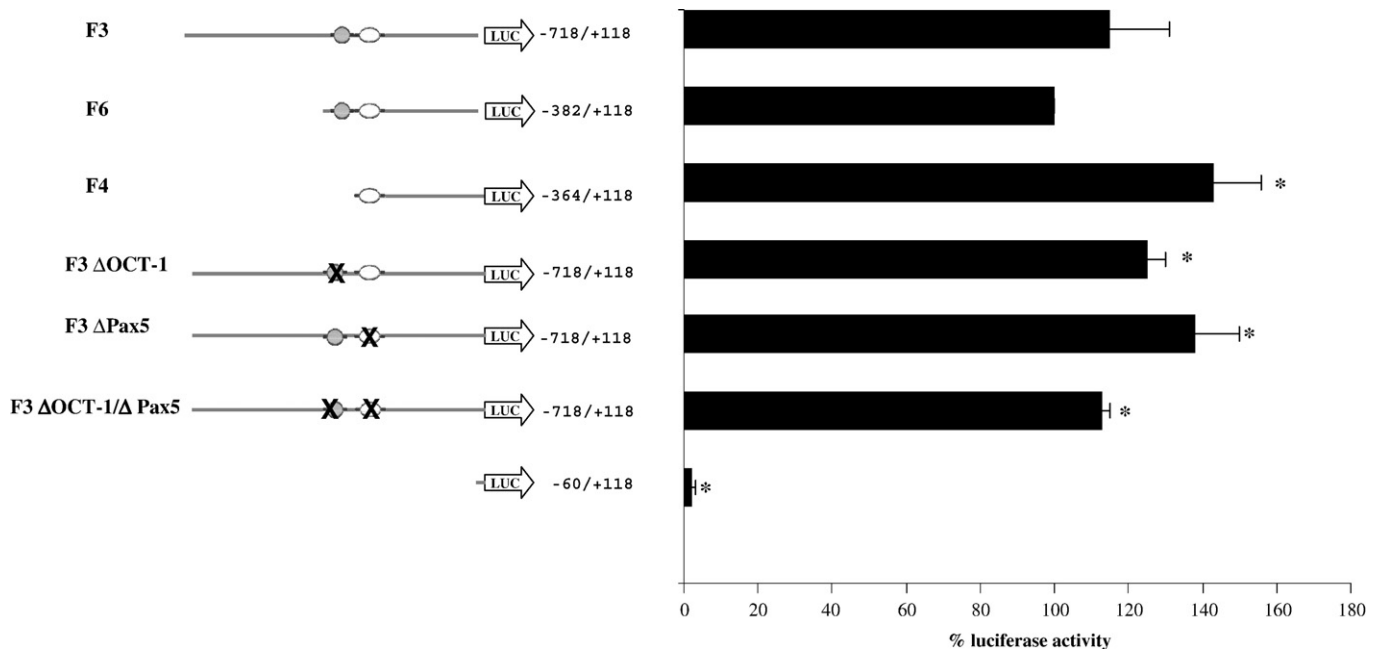

Fig. 3. 5′-deletion functional analysis of the human FDPS promoter in HeLa cells. Schematic representation of the promoter–reporter constructs containing FDPS promoter fragments of different lengths cloned into pGL3-basic vector are shown. The empty and grey coloured ovals indicate the Pax 5 and OCT-1 consensus sequences, respectively. The promoter–luciferase fusion constructs or the promoterless vector were transiently transfected into HeLa cells. Luciferase activity was normalized to *Renilla* firefly activity and expressed as % relative to the construct −382/+118, which activity is set to 100%. The results are the mean±SD from at least three independent experiments performed in triplicate.* Denotes statistically significant difference compared to the −382/+118 construct evaluated by the Student's *t* test (*p*<0.05).

human FDPS gene analyzed by the MGAlignIt algoritm, BDGP splice site predictor, ASSP and NetGen2, including the recent published results of splicing organization, is represented in Fig. 1 panels A and B. The coding sequence, organized in eleven exons, predicts a 439 aa peptide. Alternative isoforms can be derived by the presence in exon 1 and in the intron sequence between exon 2 and 3, of two alternative 5′ donor sites and 3′ acceptor sites (Fig. 1 panel B). The two ATG codons positioned in exon 2 and 3, respectively, may represent the first codon of each isoform, the mitochondrial and the cytoplasmic one. Interestingly, the complex processing of the first exon occurs as well in other organisms, where different isoforms can be identified [24,29]. Analyses in the human EST sequence databases identify two major transcripts: one including both exon 1 and intron 1, which is expressed preferentially in fetal brain tissue and another, lacking intron 1, which shows widespread expression. Human FDPS expression has been prevalently studied in cell lines, i.e. hepatic cell line, monocytic leukaemia cell line, CaCo2, HT29, K562 (human erythroleukemia cell line), human proximal tubule cell line (HK-2) and HeLa cells: these studies pointed out the regulatory expression by phorbol ester and the presence of splicing variants [25,46,47,48]. In order to integrate cell lines data we investigated the FDPS mRNA expression in human tissues by semi-quantitative RT-PCR on two panels of poly(A)$^+$RNA derived from sixteen different human tissues: heart, brain, placenta, lung, liver skeletal muscle, kidney, pancreas, thymus, spleen, prostate, testis, small intestine, ovary, peripheral blood leukocyte, colon and HeLa cells. The results are shown on Fig. 1, panel C. Relative amounts of RNA can be compared thanks to the GAPDH transcript control (one of the housekeeping genes utilized to normalize the polyA RNAs present in the panel). Initially, we analyzed the expression of FDPS mRNA utilizing primers that recognize exon 3 and exon 4 sequences which are not involved in alternative splicing, according to the "in silico" splicing analyses. In all tissues analyzed, a unique band of the expected 281 bp size was amplified (Fig. 1 panel C, FDPS F2/R1), indicating that the FDPS human gene is transcribed ubiquitously. We successively analyzed the expression of the putative alternative splicing isoforms derived by arrangements between exon 2 and 3. Using a pair of primers that overlap sequences into exon 2 and 3 (Fig. 1, panel C, FDPS F1/R21), two bands were detected. One, which is present in all tissues, corresponds to the expected 183 bp fragment; the second slower band of 260 bp derives by inclusion of a 77 bp intron between exon 2 and 3, as determined by direct sequencing of the two fragments. In the third set of amplifications, shown in panel FDPS F11/R7, we analyzed the expression of the isoforms derived by alternative processing of exon 1. Primer F11 is located 73 bp downstream the first nucleotide in the ref seq NM_002004 and deduced by genome ref seq NT_00448 relative to the first intron. This analysis showed two different amplification products that derive from the intervening sequence between exon 1 and 2 and that can be spliced using alternative 5′ donor (GT) sites and 3′ acceptor (AG) sites. An amplification product of 220 bp derived from the 712 bp intron exclusion, is well represented in all tissues. A second, less represented band of approximately 900 bp is also amplified in almost all tissues. This latter transcript derives from the 712 bp intron inclusion thereby leading to an amplification product of 932 bp. The inclusion of the 712 bp sequence in at least one of the RNA forms was confirmed by amplification of a specific fragment using an antisense primer positioned inside the intron (data not shown). The sizes of the fragments obtained by amplification were all confirmed by sequencing. These results are consistent with what reported by "Martin et al. [25]" that indicate the presence of two predominantly FDPS isoforms: a shorter cytosolic/peroxisomal form, and a longer isoform, representing the mitochondrial targeting peptide derived by alternative splicing in the first exon. Altogether these results indicate that the FDPS gene is transcriptionally expressed in all human tissues and is represented by a variety of transcripts, not equally represented.

Cloning and sequence analysis of the 5′-flanking region of the human FDPS gene

The 5′-flanking region of FDPS gene was isolated by genomic PCR, with a pair of primers spanning the sequence −718+118, respectively, derived by contig NT 004487. Sequencing of the amplified fragment allowed its alignment with the updated version in the human genome database and showed 100% identity. Computer-based analysis of the sequence using MatInspector, V2-2 software (core similarity 1, matrix similarity 0.90) using Transfac 4.0 matrices [49], revealed several putative potential *cis*-acting signals (Fig. 2, panel A). Some of them are conserved in the rat promoter sequences [30] and in the promoters of sterol regulatory element-binding protein-responsive genes, i. e. 3-hydroxy-3-methylglutaryl coenzyme A (HMG-CoA) synthase (HMGCS1), and the low density lipoprotein receptor (LDLR) and have been functionally characterized previously [32,35]. More specifically, the proximal 5′ flanking region of the FDPS gene contains: a TATA box at −128; an AP2 (activator protein 2) at position −159; a NF-Y (nuclear factor Y) at −215 and a SRE-3 at −233 that were well characterized in the rat FDPS promoter, HMG-CoA and LDLR promoters. It was demonstrated that SREBP and NF-Y may interact synergistically enhancing the transcription of the gene [34,35]. At position −269 is located an NF-Y consensus site, characterized previously in the rat promoter as a *cis*-acting signal required for normal transcriptional regulation by cellular sterols, and an YY1 consensus site is found at −239. Other putative *cis*-acting signals not previously characterized are a Pax5 binding site at position −249, a Sp1 site at position −370, an OCT-1 binding site at position −382, a more distal SP1/YY1/C-jun site at position −558, and a CAC-box at position −607. Multiple sequence alignment comparing this 5′ upstream genomic sequence of human FDPS to chimpanzee (chromosome 1 of *Pan troglodytes*), mouse (chromosome 5 of *Mus musculus*), rat (chromosome 2 of *Rattus norvegicus*) and dog (chromosome 7 of *Canis lupus familiaris*) utilizing BLAT program, identified two highly conserved regions overlapping the putative Pax5 and OCT-1
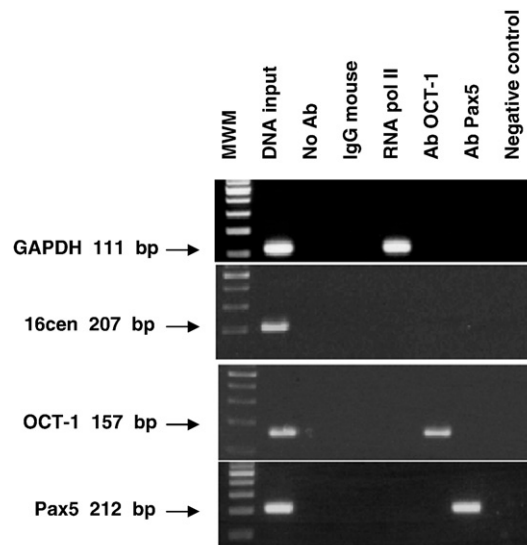

Fig. 4. Determination of OCT-1 and Pax5 binding site to the FDPS promoter by the ChIP assay. PCR amplification products obtained by DNA immunoprecipitated with antibodies (Ab) against OCT-1, Pax5, RNA pol II, non specific IgG or unimmunoprecipitated (input) from HeLa cells were analyzed into a 2% agarose gel stained with ethidium bromide. Primer pairs specific for the RNA polymerase II binding region of GAPDH promoter (positive control), 16cen (negative promote region), OCT-1 or Pax5 binding sequences of FPDS human promoter were utilized for each sample indicated on the top line, expecting fragments of the following size: 111 bp from GAPDH promoter, 207 bp from 16cen, 157 bp fragment encompassing the OCT-1-binding region of the FDPS promoter and 212 bp fragment encompassing the Pax5 binding region of the FDPS promoter. Negative control represents the PCR product in absence of template. MWM, 100 bp DNA molecular marker.

transcription factors binding sites, respectively, in the human and chimpanzee genomes, which are not present in the promoter region of the other examined orthologous genes (Fig. 2, panel B). The *in silico* analysis suggests that these two conserved regions may play a primate-bound role in the functionality of the FDPS promoter region.

Functional analyses of the human promoter of FDPS and of the contribution of two conserved cis-acting signals

To identify the sequences that are necessary for basal transcription of human FDPS, we analyzed by reporter gene assays a set of 5′ deletions of the promoter region generated by PCR of genomic sequences. The primers used for identification of the promoter activity are shown in Fig. 2, panel A (dotted arrows). The 819 bp genomic fragment was cloned 5′ to the firefly luciferase reporter gene of the pGL3-basic plasmid. The resulting plasmid pGL3 −718/+118 was used as a template for the generation of four progressively upstream deleted fragments that were cloned separately in the Promoterless luciferase vector and transiently transfected in HeLa cells.

The results of luciferase activity expressed by the reporter vectors are shown in Fig. 3 as percent relative to construct −382/+118 which contains the portion of human FDPS promoter region homologous to the functionally characterized rat FDPS promoter region [30]. Transfection of HeLa cells performed with pGL3 −718/+118, showed almost the same promoter activity of the shorter promoter sequence in −382/+118; differences in the repeated experiments of these construct, were not statistically significant. When the putative Pax5 or OCT-1 binding sites were deleted, a statistically significant ($p<0.05$) increase in activity was observed in constructs −364/+118 (+43%), ΔOCT-1 (+25%), Δ Pax5 (+38%), respectively. Deletion of both *cis*-acting sequences in construct −718/+118 ΔOCT-1/Δ Pax5 showed a 13% increase of promoter activity compared to that of −382/+118. Finally, construct −60/+118, deleted of all the putative *cis*-acting signals, showed a decrease of expression near to zero, as expected. All together these results indicate that the minimal sequence which is essential to drive transcription of FDPS with the highest luciferase activity spans nucleotides from −364 to −60 and that the putative Pax5 and OCT-1 elements modulate the activity of the promoter region.

Cellular OCT-1 and Pax 5 binding to the cognate cis-elements in the FDPS promoter

To test whether OCT-1 and Pax 5 trasncription factors bind to the FDPS promoter region we isolated and analyzed chromatin from HeLa cells by Chip assay. After immunoprecipitation with either nonspecific IgGs or with antibodies against OCT-1, Pax5, RNA pol II, respectively, PCR reactions were performed with specific primers. Using an equal amount of chromatin "input" we obtained the amplification products that are shown in Fig. 4. A 157 bp fragment containing the binding site for OCT-1 and a fragment of 212 bp containing the binding site for Pax5 were amplified from chromatin fragments immunoprecipitated with antibodies against OCT-1 and Pax5 respectively. No amplification products were obtained either by chromatin immunoprecipitated with non specific IgGs or with RNA polymerase II antibodies. These results indicate that OCT-1 and Pax 5 transcription factors do actually interact with *cis*-acting sequences in the human FDPS promoter.

Conclusions

In the present work we have reported the following results:

a) Expression of FDPS transcripts in adult human tissues: this analysis revealed that FDPS mRNAs are expressed ubiquitously, and that various splicing variants unevenly distributed in the different tissues can be detected.

b) Cloning and characterization of the FDPS promoter region and identification of the minimal promoter region: the minimal promoter located between −364 and +118 contains a TATA box and putative *cis*-acting signals that are highly conserved in orthologous genes. Further luciferase reporter expression analyses of deleted constructs indicated the presence of putative negative *cis*-acting signals between −382 and −239.

c) Identification of two conserved sequences restricted to the primate promoter region of the FDPS gene, ATAATGAAAAC at −382 and CCACAGTGC at −249 that can be recognized by OCT-1 and Pax5 transcription factors, respectively. We believe that the data presented here may add useful information for further genetic and pharmacogenetic studies, in the light of recent insights into the correlation of FDPS polymorphic variants with lipid metabolism and bone mineral density [28,50].

References

[1] R.G. Russel, Bisphosphonates: mode of action and pharmacology, Pediatrics 119 (2007) 150–162.
[2] K.L. Kavanagh, J.E. Dunford, G. Bunkoczi, R.G. Russell, U. Oppermann, The crystal structure of human geranylgeranyl pyrophosphate synthase reveals a novel hexameric arrangement and inhibitory product binding, J. Biol. Chem. 281 (2006) 22004–22012.
[3] J.L. Goldstein, M.S. Brown, Regulation of the mevalonate pathway, Nature 343 (1999) 425–430.
[4] F.P. Coxon, et al., Identification of a novel phosphonocarboxylate inhibitor of Rab geranylgeranyl transferase that specifically prevents Rab prenylation in osteoclasts and macrophages, J. Biol. Chem. 276 (2001) 48213–48222.
[5] G. Molnar, M.C. Dagher, M. Geiszt, J. Settleman, E. Ligeti, Role of prenylation in the interaction of Rho-family small GTPases with GTPase activating proteins, Biochemistry 40 (2001) 10542–10549.
[6] A.D. Basso, P. Kirschmeier, W.R. Bishop, Lipid posttranslational modifications. Farnesyl transferase inhibitors, J. Lipid Res. 47 (2006) 15–31.
[7] R.G. Russel, M.J. Roger, Bisphosphonates: from the laboratory to the clinic and back again, Bone 25 (1999) 97–106.
[8] K.L. Kavanagh, et al., The molecular mechanism of nitrogen-containing bisphosphonates as antiosteoporosis drugs, Proc. Natl. Acad. Sci. U. S. A. 103 (2006) 7829–7834.
[9] P. Masarachia, M. Weinreb, R. Balena, G.A. Rodan, Comparison of the distribution of 3H-ale dronate and 3H-etidronate in rat and mouse bones, Bone 19 (1996) 281–290.
[10] J.D. Bergstrom, R.G. Bostedor, P.J. Masarachia, A.A. Reszka, G. Rodan, Alendronate is a specific, nanomolar inhibitor of farnesyl diphosphate synthase, Arch. Biochem. Biophys. 373 (2000) 231–241.
[11] J.E. Dunford, et al., Structure–activity relationships for inhibition of farnesyl diphosphate synthase in vitro and inhibition of bone resorption in vivo by nitrogen-containing bisphosphonates, J. Pharmacol. Exp. Ther. 296 (2001) 235–242.
[12] J.E. Grove, R.J. Brown, D.J. Watts, The intracellular target for the antiresorptive aminobisphosphonate drugs in *Dictyostelium discoideum* is the enzyme farnesyl diphosphate synthase, J. Bone Miner. Res. 15 (2000) 971–981.
[13] R.K. Keller, S.J. Fliesler, Mechanism of aminobisphosphonate action: characterization of alendronate inhibition of the isoprenoid pathway, Biochem. Biophys. Res. Commun. 266 (1999) 560–563.
[14] E. van Beek, E. Pieterman, L. Cohen, C. Lowik, S. Papapoulos, Farnesyl pyrophosphate synthase is the molecular target of nitrogen-containing bisphosphonates, Biochem. Biophys. Res. Commun. 264 (1999) 108–111.
[15] M.L. Coleman, M.F. Olson, Rho GTPase signalling pathways in the morphological changes associated with apoptosis, Cell Death Differ. 9 (2002) 493–504.
[16] F.P. Coxon, M.J. Rogers, The role of prenylated small GTP-binding proteins in the regulation of osteoclast function, Calcif. Tissue Int. 72 (2003) 80–84.
[17] S. Etienne-Manneville, A. Hall, Rho GTPases in cell biology, Nature 420 (2002) 629–635.
[18] M. Zerial, H. McBride, Rab proteins as membrane organizers, Nat. Rev., Mol. Cell Biol. 2 (2001) 107–117.
[19] C.J. Sugden, J.R. Roper, J.G. Williams, Engineered gene over-expression as a method of drug target identification, Biochem. Biophys. Res. Commun. 334 (2005) 555–560.
[20] D.J. Wilkin, S.Y. Kutsunai, P.A. Edwards, Isolation and sequence of the human farnesyl pyrophosphate synthetase cDNA. Coordinate regulation of the mRNAs for farnesyl pyrophosphate synthetase, 3-hydroxy-3-methylglutaryl coenzyme A

reductase, and 3-hydroxy-3-methylglutaryl coenzyme A synthase by phorbol ester, J. Biol. Chem. 265 (1990) 4607–4614.

[21] C. Le Jossic-Corcos, C. Gonthier, I. Zaghini, E. Logette, I. Shechter, P. Bournot, Hepatic farnesyl diphosphate synthase expression is suppressed by polyunsaturated fatty acids, Biochem. J. 385 (2005) 787–794.

[22] M. Teran-Garcia, et al., Polyunsaturated fatty acid suppression of fatty acid synthase (FASN): evidence for dietary modulation of NF-Y binding to the Fasn promoter by SREBP-1c, Biochem. J. 402 (2007) 591–600.

[23] W.J. Kovacs, L.M. Olivier, S.K. Krisans, Central role of peroxisomes in isoprenoid biosynthesis, Prog. Lipid Res. 41 (2002) 369–391.

[24] N. Cunnilera, A. Boronat, A. Ferrer, The Arabidopsis thaliana FPS1 gene generates a novel mRNA that encodes a mithocondrial farnesyl-diphosphate synthase isoform, J. Biol. Chem. 272 (1997) 15381–15388.

[25] D. Martin, M. Piulachs, N. Cunillera, A. Ferrer, X. Belles, Mitochondrial targeting of farnesyl diphosphate synthase is a widespread phenomenon in eukaryotes, Biochim. Biophys. Acta 1773 (2007) 419–426.

[26] Y.X. Ding, X. Ou-Yang, C.H. Shang, A. Ren, L. Shi, Y.X. Li, M.W. Zhao, Molecular cloning, characterization, and differential expression of a farnesyl-diphosphate synthase gene from the basidiomycetous fungus Ganoderma lucidum, Biosci. Biotechnol. Biochem. 72 (2008) 1571–1579.

[27] S.K. Krisans, J. Ericsson, P.A. Edwards, G.A. Keller, Farnesyl-diphosphate synthase is localized in peroxisomes, J. Biol. Chem. 269 (1994) 14165–14169.

[28] M.E. Levy, R.A. Parker, R.E. Ferrell, J.M. Zmuda, S.L. Greenspan, Farnesyl diphosphate synthase: a novel genotype association with bone mineral density in elderly women, Maturitas 57 (2007) 247–252.

[29] J.H. Teruya, S.Y. Kutsunai, D.H. Spear, P.A. Edwards, C.F. Clarke, Testis-specific transcription initiation sites of rat farnesyl pyrophosphate synthetase mRNA, Mol. Cell. Biol. 10 (1990) 2315–2326.

[30] D.H. Spear, S.Y. Kutsunai, C.C. Correll, P.A. Edwards, Molecular cloning and promoter analysis of the rat liver farnesyl diphosphate synthase gene, J. Biol. Chem. 267 (1992) 14462–14469.

[31] D.H. Spear, J. Ericsson, S.M. Jackson, P.A. Edwards, Identification of a 6-base pair element involved in the sterol-mediated transcriptional regulation of farnesyl diphosphate synthase, J. Biol. Chem. 269 (1994) 25212–25218.

[32] S.M. Jackson, J. Ericsson, T.F. Osborne, P.A. Edwards, NF-Y has a novel role in sterol-dependent transcription of two cholesterogenic genes, J. Biol. Chem. 270 (1995) 21445–21448.

[33] J. Ericsson, S.M. Jackson, B.C. Lee, P.A. Edwards, Sterol regulatory element binding protein binds to a cis element in the promoter of the farnesyl diphosphate synthase gene, Proc. Natl. Acad. Sci. U. S. A. 93 (1996) 945–950.

[34] J. Ericsson, S.M. Jackson, P.A. Edwards, Synergistic binding of sterol regulatory element-binding protein and NF-Y to the farnesyl diphospate synthase promoter

is critical for sterol-regulated expression of the gene, J. Biol. Chem. 271 (1996) 24359–24364.

[35] J. Ericsson, A. Usheva, P.A. Edwards, YY-1 is a negative regulator of transcription of three sterol regulatory element-binding protein-responsive genes, J. Biol. Chem. 274 (1999) 14508–14513.

[36] P.D. Siebert, B.C. Huang, Identification of an alternative form of human lactoferrin mRNA that is expressed differentially in normal tissues and tumor-derived cell lines, Proc. Natl. Acad. Sci. U. S. A. 94 (1997) 2198–2203.

[37] B.T.K. Lee, T.W. Tan, S. Ranganathan, MGAlignIt : a web service for the alignment of mRNA/EST and genomic sequences, Nucleic Acids Res. 31 (2003) 3533–3536.

[38] M.G. Reese, F.H. Eeckman, D. Kulp, D. Haussler, Improved splice site detection in genie, J. Comp. Biol. 4 (1997) 311–323.

[39] M. Wang, A. Marín, Characterization and prediction of alternative splice sites, Gene 366 (2006) 219–227.

[40] S.M. Hebsgaard, P.G. Korning, N. Tolstrup, J. Engelbrecht, P. Rouze, S. Brunak, Splice site prediction in Arabidopsis thaliana DNA by combining local and global sequence information, Nucleic Acids Res. 24 (1996) 3439–3452.

[41] S. Brunak, J. Engelbrecht, S. Knudsen, Prediction of human mRNA donor and acceptor sites from the DNA sequence, J. Mol. Biol. 220 (1991) 49–65.

[42] E. Wingender, et al., The TRANSFAC system on gene expression regulation, Nucleic Acids Res. 29 (2001) 281–283.

[43] W.J. Kent, BLAT-the BLAST-like alignment tool, Genome Res. 12 (2002) 656–664.

[44] R.S. Sparkes, et al., Assignment of genes that are expressed during cholesterol synthesis to chromosomes 1q24–1q31, 15q15–15q21 and Xq13–Xq21, Cytogenet. Cell Genet. 46 (1987) 696.

[45] C. Heinzmann, et al., Dispersed family of human genes with sequence similarity to farnesyl pyrophosphate synthetase, Genomics 5 (1989) 493–500.

[46] S. Murthy, H. Tong, R.J. Hohl, Regulation of fatty acid synthesis by farnesyl pyrophosphate, J. Biol. Chem. 280 (2005) 41793–41804.

[47] H. Tong, A.J. Wiemer, J.D. Neighbors, R.J. Hohl, Quantitative determination of farnesyl and geranylgeranyl diphosphate levels in mammalian tissue, Anal. Biochem. 378 (2008) 138–143.

[48] A. Lühe, K.P. Künkele, M. Haiker, K. Schad, C. Zihlmann, F. Bauss, L. Suter, T. Pfister, Preclinical evidence for nitrogen-containing bisphosphonate inhibition of farnesyl diphosphate (FPP) synthase in the kidney: Implications for renal safety, Toxicol. In Vitro 22 (2008) 899–909.

[49] K. Quandt, K. Frech, H. Karas, E. Wingender, T. Werner, MatInd and MatInspector: new fast and versatile tool for detection of consensus matches in nucleotide sequence data, Nucleic Acids Res. 23 (1995) 4878–4884.

[50] M.A. Wollmer, et al., Association study of cholesterol-related genes in Alzheimer's disease, Neurogenetics 8 (2007) 179–188.